



# The combined effectiveness of activated carbon (AC) / ZnO for the adsorption of mebeverine hydrochloride / photocatalytic degradation under sunlight

Assia Djebri<sup>1</sup> · Mohamed Belmedani<sup>2</sup> · Badreddine Belhamdi<sup>3</sup> · Mohamed Trari<sup>4</sup> · Zahra Sadaoui<sup>1</sup>

Received: 28 November 2020 / Accepted: 7 January 2021 / Published online: 23 January 2021  
© Akadémiai Kiadó, Budapest, Hungary 2021

## Abstract

The photocatalytic degradation of the Mebeverine hydrochloride (MEB) by ZnO and the combined ZnO-Activated Carbon (ZnO-AC) under solar light has been investigated in batch mode. The AC was prepared from dates stems using  $\text{ZnCl}_2$  as chemical activation agent. The effect of some operating parameters on the MEB degradation efficiency such as: photocatalyst dose, solution pH and initial MEB concentration has been examined. The results revealed that the surface reaction on ZnO plays a crucial role in the MEB photo-degradation as confirmed by UV-Visible spectrophotometry. The photocatalytic efficiency of the mixture ZnO-AC is dependent on the mass ratio ZnO/AC, which was optimized for a value of 15 wt%. The MEB degradation kinetics follows a pseudo first order model and the Langmuir-Hinshelwood (L-H) model fit adequately the experimental data. Besides, our results show that the combined system (adsorption/photocatalysis) is effective for the MEB degradation than the photocatalysis process alone. A comparative study with the literature indicated the benefits of coupling ZnO-AC under the solar light ( $93 \text{ mW cm}^{-2}$ ).

**Keywords** Dates Stems · Activated Carbon · Mebeverine Hydrochloride · ZnO · Photocatalysis · Solar light

---

**Supplementary Information** The online version of this article (doi:<https://doi.org/10.1007/s11144-021-01932-x>) contains supplementary material, which is available to authorized users.

---

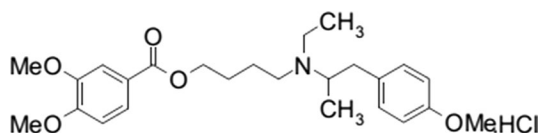
✉ Mohamed Trari  
mtrari@usthb.dz

Extended author information available on the last page of the article

## Introduction

The extensive use of pharmaceutical drugs has resulted in frequent detection of their residues in the aquatic medium through many sources. They have been found in soil, surface and waste water and even in drinking water at levels up to few  $\mu\text{g L}^{-1}$ . Therefore, an increasing attention has been directed toward the pharmaceutical industry as a source of the environmental pollution, with major concerns about its harmful impact on the ecosystem and public health [1, 2]. A lot of unused, expired and residual drugs have been discharged into the aquatic environment during and after treatment [3, 4] and are often excreted into sewage with metabolite as well as the unchanged parent compounds [5, 6]. In order to limit this eco-toxicological risk, several projects are looking for strategies to limit the water pollution by pharmaceutical products. In this study, Mebeverine Hydrochloride (MEB) was chosen as pollutant; the chemical structure, molecular weight and formulae are given in Fig. 1. It is a musculotropic anti-spasmodic agent employed in a variety of conditions and affects the vascular system as well as the gastro-intestinal and genitor-urinary tracts. Conventionally, the adsorption reduces the pollution but not enough to reach the level required by the directives of the water standards [7, 8]. At this level, the photocatalysis takes over and is suggested as a clean and inexpensive strategy to be applied at the end of the chain for the water treatment. In addition, coupling the adsorption with photocatalysis was tentatively attempted for the removal of hazardous compounds and the combined methods have been found effective for the drugs degradation [9, 10]. To our knowledge, this contribution is among the first study that reports the adsorption/photocatalysis coupling for the MEB elimination. Indeed, no research works are currently known regarding the coupling processes, and the oxidation of pharmaceuticals compounds using ZnO-AC under solar light which constitutes the aim of this work. In addition, the kinetic study of the MEB degradation as well as the involved mechanism induced upon solar irradiation, were investigated. Indeed, the current research provides new data of the adsorption/photocatalytic process of the MEB elimination from water.

**Fig. 1** Chemical structure, molecular weight and molecular formula of mebeverine hydrochloride (MEB)



MEB  
mol wt 466.02  
 $\text{C}_{25}\text{H}_{35}\text{NO}_5 \cdot \text{HCl}$

## Experimental

### Preparation of the activated carbon (AC)

Dates stems were provided from the southern Algeria; the raw material was thoroughly washed with distilled water to remove dirt; it was cut into 1–2 mm particle size, dried at 60 °C, milled and then screen-sieved. The chemical activation of the precursor was performed by using  $\text{ZnCl}_2$  as chemical agent. 20 g of  $\text{ZnCl}_2$  were dissolved in 100 mL of distilled water and 10 g of raw material was impregnated with  $\text{ZnCl}_2$  solution (activating agent/ raw material: 1/1). The mixture was stirred during 4 h at 70 °C and the sample was dried at 110 °C ( $\pm 2$  °C) until complete evaporation. Subsequently, the impregnated sample was activated in a tubular furnace at 500 °C at a heating rate of 10 °C/min for 2 h and cooled to room temperature. Then, the material was removed, washed, with HCl solution (0.5 N) and hot distilled water several times until reaching pH~7. Finally, the powder was heated in an oven at 105 °C ( $\pm 2$  °C) overnight and stored in hermetic bottles for further use.

### Characterization techniques

A Fourier Transformed Infrared Red Spectrometer (FTIR, Perkin Elmer) was used to identify the functional groups on the AC surface using dried KBr of spectroscopic quality. The FTIR spectrum was recorded at room temperature from 4000 to 400  $\text{cm}^{-1}$ .

The point of zero charge (pzc) at which the charge of the adsorbent surface is zero was determined by the method described in the literature [11].

### Reagents and analysis

The Mebeverine Hydrochloride (MEB) was provided by SAIDAL Company (Algiers) and all the chemicals were of an analytical grade quality. The pH of the solutions was adjusted by addition of NaOH or HCl. The MEB concentration was determined with a UV-Visible spectrophotometer (model Specord 200) at the maximum absorption ( $\lambda_{\text{max}} = 265$  nm), using 1 cm quartz cell. The MEB concentrations from aqueous solutions were determined by linear interpolation of the calibration curve.

### Photocatalytic experiments

#### Photocatalytic and photolytic degradation

The tests were performed in a Pyrex reactor open to atmosphere. The catalyst was suspended in MEB solution (200 mL) by magnetic stirring for 3 h in the dark to reach the adsorption equilibrium. Then, the reactor was exposed to solar light

(93 mW cm<sup>-2</sup>) to perform the photodegradation tests. The aliquots (3 mL) were collected at fixed time intervals, filtered off through a membrane filter (pore size 0.45 μm) and analyzed by spectrophotometry UV-Visible.

### Coupling adsorption/photocatalysis processes

The activity of the combined processes (adsorption/photocatalysis) was assessed by varying the proportion of ZnO (ZnO/AC referred by x = 15, 35, 50 and 70 wt%). First of all, AC and ZnO were prepared separately to obtain 1 g of the mixture. The mixture (ZnO-AC) ratio was magnetically dispersed in MEB solutions at different initial concentrations. The photocatalytic reactions were carried out in batch mode under solar light; this allowed us to establish the experimental protocol and to realize both processes (adsorption/photocatalysis) in the same time within 30 min of irradiation. For the kinetic study, the samples (5 mL) were collected at regular times for analysis.

### Estimation of the analysis error

An error function assessment is required in order to evaluate the fit of the equations to the experimental results. To determine the best fit model for the photocatalytic degradation, the derived linear and non-linear equations of each model fitting by the software Origin Pro 8.5, were employed to simulate and to confirm the fitting of the photocatalytic degradation kinetic model to the experimental data. In the present study, the statistical significance of variables was evaluated from the analysis of the sum of errors squared (SSE) and average relative error deviation (ARED). The best fit of the experimental data is indicated by the lower values of the SSE and ARED functions.

$$SEE = \sum (C_{t,cal} - C_{t,exp})^2 \quad (1)$$

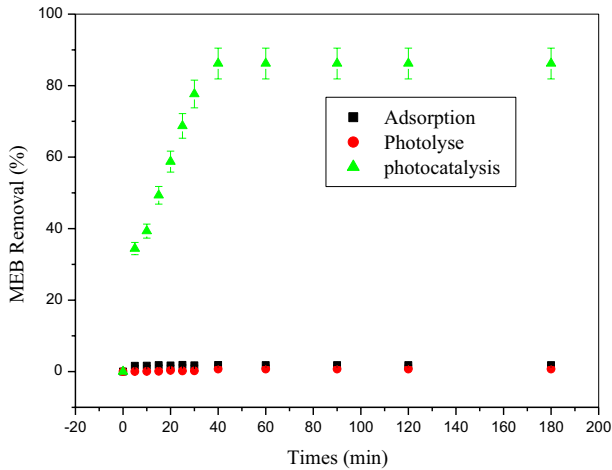
$$ARED = \frac{1}{N} \sum \left( \frac{C_{t,cal} - C_{t,exp}}{C_{t,cal}} \right) 100 \quad (2)$$

where the subscripts (exp) and (cal) are the experimental and the calculated values of the residual MEB concentration C (mg/L) and N, is the measurements number.

## Results and discussion

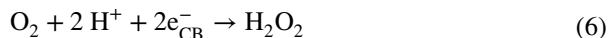
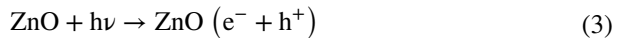
### Photocatalytic MEB degradation

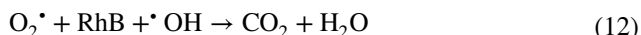
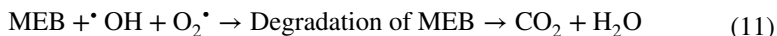
Tests of the dark adsorption and photolysis (without catalyst) under sunlight were carried out in order to quantify the contribution of each process on the MEB removal. The study was realized at pH 6.6 with MEB initial concentration of 21.45 mg/L and catalyst dose of 0.4 g/L. As illustrated in Fig. 2, the MEB removal



**Fig. 2** The MEB photo-degradability ([MEB] = 21.45 mg/L, pH ~ 6.6 ZnO dose = 0.4 g/L)

by photolysis and adsorption is practically insignificant. Conversely, in the presence of ZnO as sensitizer, a rapid degradation of MEB occurred under solar irradiation and the significant change in the MEB removal is mainly due to the photocatalytic process. The electrons are excited to ZnO-CB and a good performance is observed under solar light (UVA) where 86% of MEB was removed after 40 min of irradiation (Fig. 2). This result is due to light induced MEB mineralization. The possible reactions occurring at the interface are the following:





This indicates that the potential of the couple  $\text{O}_2/\text{O}_2 \cdot$  is above ZnO-CB ( $-1.5$  V) and contributes in the MEB oxidation. Concomitantly, the holes permit the oxidation of water into oxygen, resulting in prolonged life-time of electron/hole ( $e^-/h^+$ ) pairs since the level of the  $\text{O}_2/\text{H}_2\text{O}$  couple is more anodic than ZnO-CB. The Mott-Schottky ( $C^{-2} - E$ ) characteristic of ZnO plotted in neutral solution (Fig. S1) gives a flat band potential of  $-056$  V:

$$C^{-2} = \frac{2}{\epsilon\epsilon_0 A^2 e N_D} (E - E_{\text{fb}}) \quad (11)$$

The symbols have their usual significations. Therefore, the valence band (VB) and conduction band (CB) are given by:

$$E_{\text{CB}} = 4.75 + eE_{\text{fb}} - E_a \quad (12)$$

$$E_{\text{VB}} = E_{\text{CB}} - E_g \quad (13)$$

## Kinetic study of MEB degradation by solar light/ZnO system

### Effect of initial MEB concentration

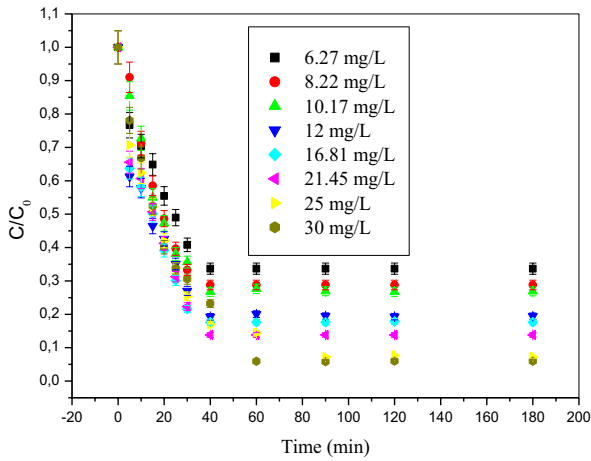
The effect of the initial MEB concentration ( $C_0$ ) on the photo degradation process was investigated in the concentrations range of 2–30 mg/L for catalyst dose of 0.4 g/L and pH 6.6. The kinetic results (Fig. 3) show the dependence of the MEB removal with the initial concentration. The life time of  $\cdot\text{OH}$  and  $\text{O}_2 \cdot$  radicals is very short (only few nanoseconds) and can react only near the catalyst surface where they are formed. For high  $C_0$  values, the number of MEB molecules, enhance the probability of their collision with radicals, thus leading to an increased degradation rate [12]. The photodegradation of MEB is well described by a pseudo first order kinetics:

$$-\frac{dC}{dt} = k_{\text{ap}} C \quad (14)$$

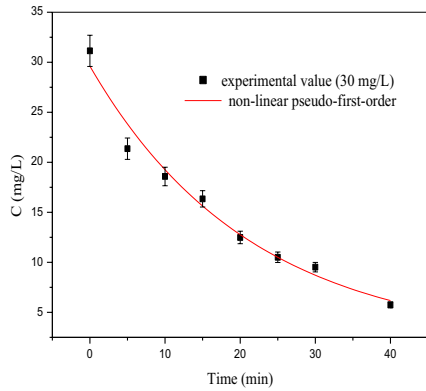
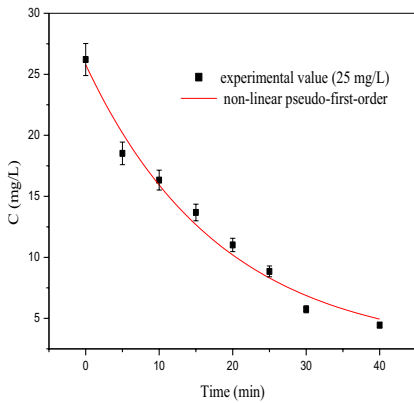
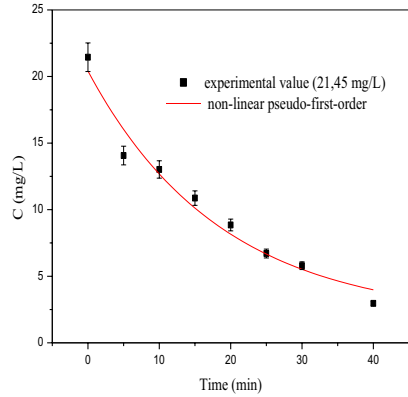
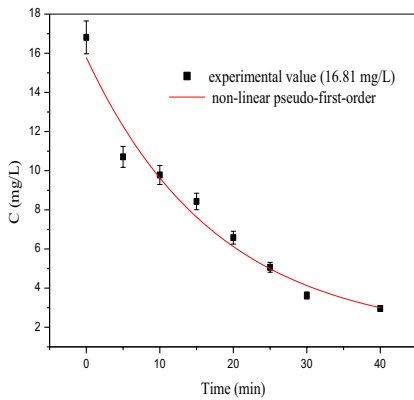
$k_{\text{ap}}$  ( $\text{min}^{-1}$ ) is the apparent rate constant. The integration of Eq. 14 (with the same restriction of  $C = C_0$  at  $t = 0$ ) leads to the following relation:

$$\ln\left(\frac{C_0}{C}\right) = k_{\text{ap}} t \quad (15)$$

This indicates that a plot of  $\ln(C_0/C)$  versus  $t$  for different MEB concentrations should be linear with slope equal to  $k_{\text{ap}}$  which can be evaluated by linear least-squares analysis.



(a)



(b)

**Fig. 3** (a) The MEB photocatalytic degradation, (b) The MEB degradation rate, at different initial concentrations (ZnO dose = 0.4 g/L, pH ~ 6.6, T = 25 °C)

To evaluate  $k_{ap}$  by linear least-squares analysis requires that  $C_0$  must be known in advance. Small errors in  $C_0$  can cause large errors in  $k_{ap}$  value because of the increasing error in the logarithm of the difference ( $C_0 - C_t$ ). The defect in applying Eq. 15 is that the values are not equally reliable. Consequently a more effective method for fitting all such data to first order kinetics is non-linear least-squares analysis using Eq. 16 [13–15]:

$$A = Xe^{(-k_{ap}t)} + E \quad (16)$$

Here  $A$  is the MEB calculated residual,  $X$ , is the amplitude of the process,  $k_{ap}$ , is the pseudo-first order rate constant, and  $E$ , is the end point. The results from the Fig. 4 prove that the MEB photodegradation kinetics follows adequately the pseudo-first order kinetic model. In order to elucidate the involved mechanisms for the MEB degradation; recent researches have reported the photooxidation of organic pollutants, which obey the Langmuir–Hinshelwood (L–H) model [16–19]:

$$r_0 = k_r \frac{K_{L-H}C_e}{1 + K_{L-H}C_e} \quad (17)$$

Here,  $r_0$  (mg/L.min), is the initial rate of the photocatalytic degradation,  $K_{L-H}$  (L/mg), the adsorption equilibrium constant and  $k_r$ , a constant depending on the physical factors like the UV photons flux and catalyst dose. Eq. 17 can be modified as follows [20]:

$$\frac{C_e}{r_0} = \frac{1}{k_r K_{L-H}} + \frac{1}{k_r} C_e \quad (18)$$

The applicability of the L–H model for the MEB degradation is confirmed by the straight line of the plot  $C_e/r_0 = f(C_e)$  (Fig. S2). The values of  $k_r$  (3.07 mg/L min)

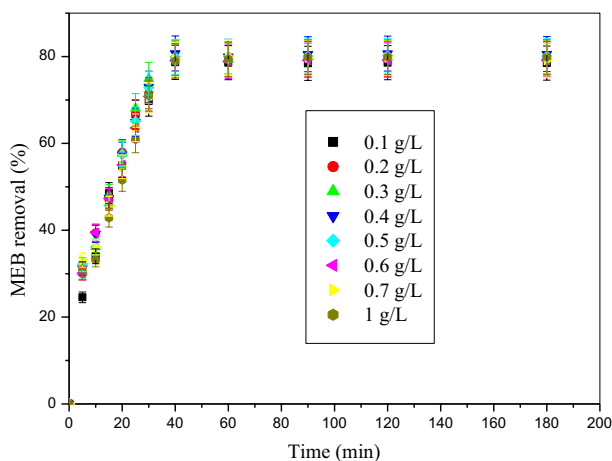


**Fig. 4** The effect of ZnO dose on the MEB photodegradation ([MEB] = 12.16 mg/L, T = 25 °C, pH = 6.5)



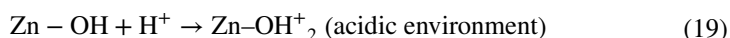
and  $K_{L-H}$  (0.575 L/mg) are deduced from the slope and intercept of the curve. These results are of the same order of magnitude than those reported elsewhere [21, 22]. The L–H model based on the attack by the radicals  $\bullet\text{OH}$  and  $\text{O}_2\bullet$  was developed to interpret the experimental data, the good correlation coefficient ( $R^2=0.999$ ) shows that the MEB oxidation by  $\bullet\text{OH}$  radicals, remains predominant. The results illustrated in Table 1, indicate an increase of the initial rate  $r_0$  with the MEB initial concentration which is in agreement with the L–H model.

### Effect of ZnO dose

In this section, the experiments were performed by varying the ZnO dose in the range of 0.1–1 g/L at pH (6.5). As expected, from the Fig. 4, the results show that increasing the catalyst dose enhances the MEB removal efficiency. Such behavior is due to the high number of active sites which leads to an increase in the number of  $\bullet\text{OH}$  radicals, leading to a greater interaction with the MEB molecules. An optimal ZnO dose of 0.4 g/L is obtained for an initial MEB concentration of 12.16 mg/L within 40 min of solar irradiation. However, further increase of ZnO saturates the surface area and the number of photoactive sites remains almost constant. This can also be due to the dispersion of light as well as the sedimentation and agglomeration of ZnO [23, 24]. The light scattering also accounts for the constancy of the activity.

### Effect of solution initial pH

Generally, the pH has a great influence of the solution and is crucial in photocatalysis; it affects the electrical charge of the photocatalyst which governs the ionization state of its surface. The point of zero charge ( $\text{pH}_{\text{pzc}} \sim 9$ ) indicates that the ZnO surface is positively charged for  $\text{pH} < \text{pH}_{\text{pzc}}$  (Eq. 19), and negatively above  $\text{pH}_{\text{pzc}}$ :



The experiments were conducted in the pH range of 3.4–7.5, maintaining the other parameters constant. From Fig. 5, curiously and contrary to what it is expected, the MEB oxidation is not affected by the solution pH. Therefore, such behavior cannot be explained in terms of ZnO charge and ionization state of the MEB molecule. Thus, the positive holes ( $h^+$ ) in the valence band (VB) are among the major oxidation species at low pH values, while at high pH, the  $\bullet\text{OH}$  radicals are considered the dominant species [25, 26]. So, the MEB degradation is controlled by the photo holes rather than radicals. The best degradation was obtained at free pH ( $\sim 6.5$ ),

**Table 1** Kinetic data obtained by the non-linear regression of the pseudo-first order model for the MEB photocatalytic degradation by solar light /ZnO system

$C_0$ (mg/L)	$k_{\text{app}}$ ( $\text{min}^{-1}$ )	$r_0$ (mg/L min)	$R^2$	SEE	ARED
16,81	$5.6 \times 10^{-2}$	1.22	0.967	4.64	6.711
21,45	$4.6 \times 10^{-2}$	1.48	0.971	6.042	8.558
25	$5.4 \times 10^{-2}$	1.54	0.981	5.375	5.996
30	$4.6 \times 10^{-2}$	1.96	0.977	7.37	6.061

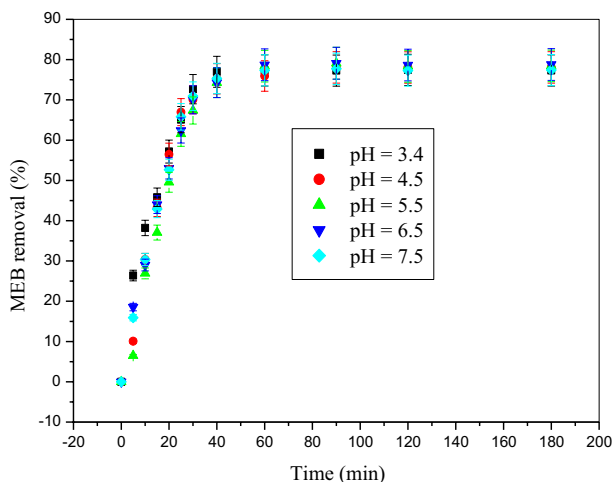


**Fig. 5** The effect of the solution initial pH on MEB photodegradation ( $[\text{MEB}]_0 = 10.74 \text{ mg/L}$ ,  $\text{ZnO}$  dose =  $0.4 \text{ g/L}$ ,  $T = 25 \text{ }^\circ\text{C}$ )

close to the natural environment. Let's recall that the ZnO electronic bands vary from  $-0.059 \text{ V pH}^{-1}$ , this allowed us to locate them in a potential diagram at  $\text{pH} \sim 7$ .

According to the proposed mechanism diagram of MEB photocatalysis presented previously, the oxidation of organic matter in solution is initiated by the photoexcitation of ZnO, with the formation of an electron–hole ( $e^-h^+$ ) pairs (Eq. 3). The high oxidative potential of the holes ( $h^+_{\text{VB}}$ ) permits the direct oxidation of MEB to reactive intermediates. The  $\bullet\text{OH}$  radicals can be formed either by the water decomposition (Eq. 4) or by oxidation of  $\bullet\text{OH}$  (Eq. 8). Concomitantly, the electrons in the conduction band ( $e^-_{\text{CB}}$ ) can reduce molecular oxygen to superoxide anion  $\text{O}_2^\bullet$  (Eq. 7) which in presence of organic scavengers may form organic peroxides (Eq. 6) or  $\text{H}_2\text{O}_2$  (Eq. 10).  $\bullet\text{OH}$  species have been indicated as the first responsible of the mineralization of organics [27, 28].

### FT-IR spectra of ZnO

MEB can be mineralized or transformed to a metabolite. In order to clarify the degradation mechanism, the structure of ZnO before and after MEB degradation was analyzed by the FT-IR spectroscopy. Apparently, no significant change was noticed in the absorption spectrum after degradation (Fig. S3). The absence of new bands clearly indicates that the MEB is mineralized into  $\text{H}_2\text{O}$  and  $\text{CO}_2$ . Metal oxides give absorption bands below  $1000 \text{ cm}^{-1}$ . Therefore, the peaks at  $428$ ,  $440$ ,  $447 \text{ cm}^{-1}$  are assigned to Zn-O.

### Coupling of adsorption/ photocatalysis processes

The photocatalysis can be improved by exploiting the physical properties of activated carbons, because of their large specific surface area, which is usually attributed

to the increased contact AC/MEB which is favored by the porous nature of the activated carbons [29–32]. However, some carbons play more than just a supporting role, as shown by recent studies [33, 34] where 80% of the phenol mineralization was achieved by photooxidation under UV radiation in the presence of the activated carbon. The specific objective of this section was to study the MEB degradation by the photo-system (solar light/ZnO-AC) and to elucidate the role of the AC physical and chemical properties.

## MEB degradation by the (solar light/AC-ZnO) system

### Effect of the (ZnO/AC) ratio

The heterogeneous solar photocatalysis is an emergent alternative to remove inorganic pollutants and further mineralize the organic molecules. In order to determine whether the AC truly maintains the photoactive properties, we studied its capacity for the MEB oxidation. For this purpose, the experiments were performed by varying the mass ratio  $m_{AC}/m_{ZnO} = x$ , with  $x = 15, 35, 50$  and  $70$  wt% for MEB initial concentration of  $30$  mg/L and pH  $6.5$ . The experiments focus on the combined adsorption/photocatalysis and the results from Fig. 6, showed an enhancement of the MEB removal efficiency with decreasing the (ZnO/AC) mass ratio suggesting the activated carbon contribution to the overall MEB removal. These results are consistent with the ability of the activated carbon to promote photocatalysis in which the AC itself acts as a porous support [26, 28]. Indeed, the activated carbon acts as templating agent by monitoring both the AC surface area and the ZnO particles morphology which are directly related to the surface electrons of the AC. The role of AC in the degradation was quantified in terms of the synergy factor (SF) i.e. the

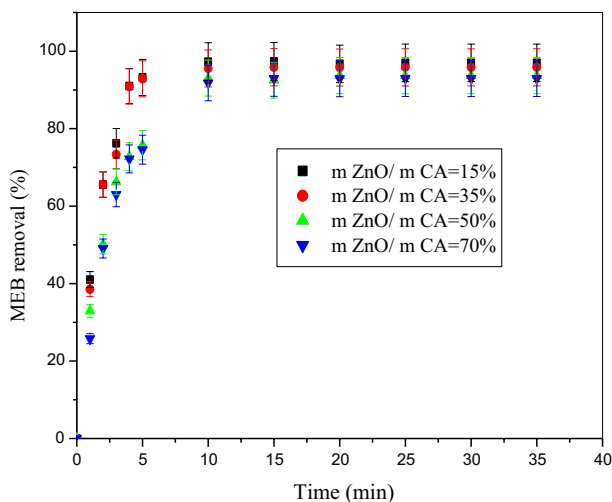


**Fig. 6** The influence of (ZnO-AC) ratio on the MEB photo-degradation efficiency ( $[MEB]_0 = 29,6$  mg/L,  $T = 25$  °C,  $pH = 6.5$ )

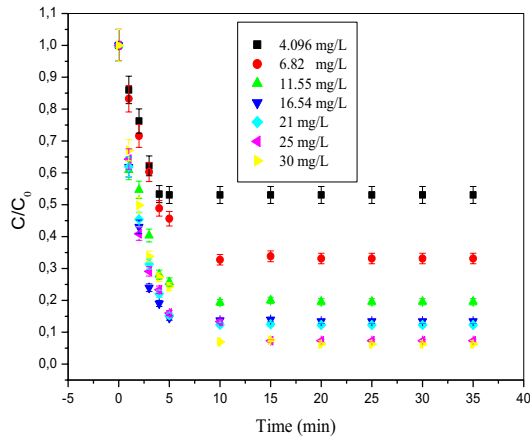
ratio of the photocatalytic rate constant in the presence of the AC ( $k_{\text{ZnO-AC}}$ ) to that without the AC ( $k_{\text{ZnO}}$ ) [35, 36]:

$$SF = k_{\text{ZnO-AC}}/k_{\text{ZnO}} \quad (20)$$

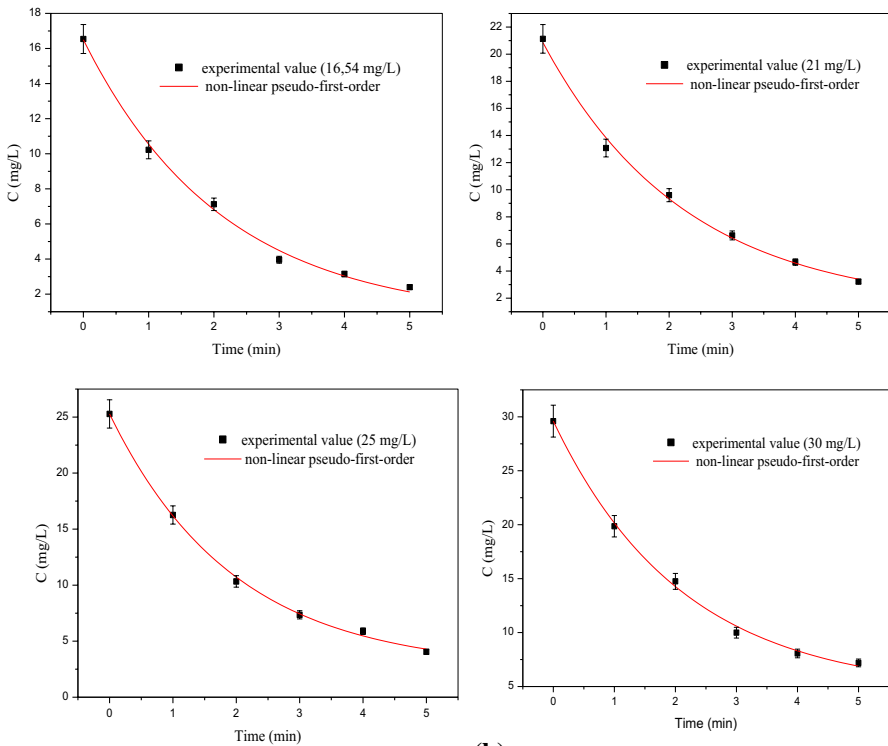
The synergy factor SF, which is derived from the apparent first order rate constant is equal to 7.5 ( $SF \gg 1$ ), indicating that AC exerts a high synergic effect on the MEB degradation by the solar light/ZnO-AC system because of the large interfacial contact ZnO-AC which has advantages over simple mixtures [37]. The optimal value of the ZnO/AC mass ratio is found to be 15% for a MEB initial concentration of 30 mg/L under solar light irradiation of  $930 \text{ mW cm}^{-2}$ .

### Effect of the initial MEB concentration

The real effluents contain pollutants at different concentrations ranging up to  $30 \text{ mg L}^{-1}$  or more and it is instructive to study the effect of the MEB initial concentration ( $C_0$ ) on the photo activity which affects directly the coverage of the catalyst surface. The MEB photo-oxidation by the ZnO-AC system is higher than by ZnO. Indeed, from the results illustrated on the Fig. 7, high degradation rates of MEB were observed during the first 5 min of irradiation. This is due to the free surface of the AC at early stage, which led to a higher adsorption capacity of the catalyst and the abundance of  $\bullet\text{OH}$  radicals near the surface. This shows that ZnO-AC system does not only attain a higher MEB degradation efficiency but also accelerates the photocatalytic process. Apparently, the combined process enhances the reaction between  $\bullet\text{OH}$  and MEB molecules because of the MEB molecules attraction to the active sites on the catalyst surface at pH 6.5. Moreover, the degradation efficiency is attributed to the affinity to the binding sites for the ZnO-AC system. The MEB degradation increases with initial concentration and no inhibition of the catalyst is observed. In addition, ZnO is able to absorb more light without provoking great light scattering effect [39], which can be proved by the enhanced removal efficiency with raising MEB initial concentration. After only 5 min, the degradation reached 97% for MEB initial concentration of 30 mg/L, showing the performance and synergy of the activated carbon. For high concentrations, the ZnO-AC surface is saturated by the MEB molecules and the kinetic model obeys zeroth order kinetics, which implies that the rate does not depend on the external mass transfer. On the contrary, for low MEB initial concentrations, the kinetics follows a pseudo-first order model and the overall rate is concentration independent in the range of 2–30 mg/L. It depends on the mass transfer [38] on the ZnO-AC system ratio (15%) as shown in Fig. 6. Moreover, the high correlation coefficient ( $R^2=0.99$ ) revealed that the photodegradation follows the L-H model. The parameters of this photocatalytic reaction are confirmed by the linear plot of  $C_0/r_0 = f(C_0)$  (Fig. S4) with the constants  $k_r=12.5 \text{ mg/L}\cdot\text{min}$  and  $K_{\text{L-H}}=0.01224 \text{ L/mg}$ . Similar results were reported by Cordero-Garcia et al. [40] and Rojas et al. [41]. The results of the application of the non linear relationship (Eq. 16) are illustrated in Fig. 7 (b). The constant  $k_{\text{app}}$ , initial degradation rate ( $r_0$ ) and correlation coefficient  $R^2$  are gathered in Table 2.



(a)



(b)

**Fig. 7** (a) The Photocatalytic MEB degradation, (b) The MEB degradation rate, at different initial concentrations ((ZnO-AC) ratio = 50%, pH ~ 6.6, T = 25 °C)

**Table 2** Kinetic data obtained by the non-linear regression of the pseudo-first order model for the MEB photocatalytic degradation by solar light / ZnO-CA system

$C_0$ (mg/L)	$k_{app}$ ( $\text{min}^{-1}$ )	$r_0$ (mg/L min)	$R^2$	SEE	ARED
16.54	0.469	6.314	0.996	0.558	5989
21	0.445	8.055	0.996	0.793	3261
25	0.510	9.017	0.998	0.396	3084
30	0.472	9.744	0.997	0.836	2979

### Proposed MEB photocatalytic mechanism by solar light/ZnO-AC system

Activated carbon possesses a high number of active adsorption sites owing to its well-developed porous structure with a very large surface area and a high adsorption capacity. Thus, MEB is adsorbed onto the AC before being transferred to the photocatalytic sites of ZnO [43, 44]. ZnO particles are hydrophilic when exposed to solar light whereas the MEB molecules are hydrophobic. The AC provides active sites for an effective photodegradation onto ZnO. The MEB concentration is high on ZnO and the reaction rate is faster. Additionally, the activated carbon functional groups are hypothesized to interact coordinatively with photocatalytic sites located on ZnO surfaces. Coordination of ZnO sites with oxygen-containing activated carbon-functional surface groups enables the transfer of electrons between photocatalyst and adsorbent [42]. Ania et al. [43] assumed that photo-induced mobile electrons in the photocatalyst can be transferred to the neighbouring activated carbon surface in this way. The surface chemistry (and therefore the source material and the activation process) of the activated carbon affects both the photocatalyst/activated carbon interfacial area and the charge (electron or hole) transfer between the two solids [43]. Therefore, only particular activated carbons cause synergetic effects in the ZnO/activated carbon combination process. Combined ZnO-AC, as sensitizer is an approach to develop photocatalyst responsive to UV light and the MEB degradation by ZnO-AC system is determined by the support AC. Thus, the system absorbs the  $UV_A$  photons, and the excited electrons from ZnO-VB to ZnO-CB, generate electron-hole ( $e^-/h^+$ ) pairs. The holes in the VB can form  $\bullet\text{OH}$  radicals through the oxidative reactions (See Sect. 3.1.), while the electrons in CB can generate super oxide  $\text{O}_2^{\bullet-}$  (Eqs. 7–9). Both  $\bullet\text{OH}$  and  $\text{O}_2^{\bullet-}$  are powerful oxidants for organic compounds.  $\text{O}_2^{\bullet-}$  has sufficient anodic potential (1.3 V) to oxidize organic species with electron-donating groups such as  $-\text{N}=\text{N}-$  bond while  $\bullet\text{OH}$  (2 V) tends to adsorb hydrogen or attack unsaturated  $\text{C}=\text{C}$  bonds [44]. In the presence of  $\bullet\text{OH}$  species, the degradation of MEB occurred quickly.

### Compared FT-IR spectra of ZnO and ZnO-AC system

The modification of the surface was highlighted by the FT-IR spectroscopy, a powerful technique to identify the presence of functional groups and their coordination between the activated carbon functional groups and ZnO. Generally, the absorption of inorganic oxides occurs at wave numbers below  $1000\text{ cm}^{-1}$ . Fig. S5 displays the spectra of ZnO

and ZnO-AC system before MEB degradation. From the Fig. S5a, the peaks below  $700\text{ cm}^{-1}$  are assigned to ZnO [45]. No significant peaks were observed between the ranges ( $1200\text{--}1990\text{ cm}^{-1}$ ), ( $2000\text{--}2900\text{ cm}^{-1}$ ) and ( $3000\text{--}3390\text{ cm}^{-1}$ ). However, from the Fig. S5b, for the ZnO-AC system, some peaks were observed in these regions. The broad bands in the range ( $3000\text{--}3390\text{ cm}^{-1}$ ) are assigned to -OH group [46]. These peaks are absent in ZnO suggesting the presence of the AC as it can absorb water unlike pure ZnO and this shows a good interaction between AC and ZnO. In order to clarify more the degradation mechanism, the structure of ZnO-AC system before and after MEB degradation was analyzed by the FT-IR spectroscopy, the obtained results are reported in the Fig. S6. From the FTIR spectrum of (ZnO-AC) system (Fig. S6), it could be seen that there is practically no change in the spectral pattern before and after MEB degradation. The spectra are similar, indicating that the functional groups were remained for the (ZnO-AC) system after MEB degradation and confirm clearly the MEB degradation.

## Conclusion

The photocatalytic MEB degradation has been studied under solar light by using ZnO and ZnO-AC catalyst systems. The effect of the catalyst dose, MEB initial concentration, solution pH, has been investigated. The results revealed maximum MEB degradation of 94% degradation under solar light/ZnO system has been achieved in a relatively short time (40 min) for the catalyst dose of 0.4 g/L and for MEB initial concentration of 30 mg/L. The results indicated that the degree of degradation was affected by the MEB concentration and ZnO dose, however, the elimination rate is not influenced by the solution pH. Otherwise, the MEB degradation results under solar light/ZnO-AC system demonstrate an improvement of MEB removal (97%) which was achieved after a very short time (5 min) relatively to the ZnO system. Indeed, the results indicated that the combined ZnO-AC system may be a viable alternative and a new way to increase the MEB photodegradation. The Langmuir–Hinshelwood model fits adequately the experimental data for the two systems investigated. The kinetic degradation follows a pseudo-first order model. The presence of the activated carbon during the MEB photodegradation process markedly increases the degradation rate. The results indicated that activated carbon exerts a greatest synergy on MEB removal by the ZnO-AC system. The MEB oxidation onto ZnO-AC system shows high reaction rates compared to ZnO and this confirms the enhanced performance of the combined system.

**Acknowledgements** The authors thank the Directorate General of Scientific Research for the encouragement. We would like to thank the colleagues that have contributed, from far or near, to the best running and carrying out of this research work.

## References

1. Kasprzyk-Hordern B, Dinsdale RM, Guwy AJ (2009) The removal of pharmaceuticals, personal care products, endocrine disruptors and illicit drugs during wastewater treatment and its impact on the quality of receiving waters. *Water Res* 43:363–380

- Gros M, Petrovic M, Barceló D (2009) Tracing pharmaceutical residues of different therapeutic classes in environmental waters by using liquid chromatography/quadrupole-linear ion trap mass spectrometry and automated library searching. *Anal Chem* 81:898–912
- Kühne M, Ihnen D, Möller G, Agthe O (2000) Stability of tetracycline in water and liquid manure. *J Veterinary Med Ser A* 47:379–384
- Zhang X, Wu F, Wu X, Chen P, Deng N (2008) Photodegradation of acetaminophen in TiO<sub>2</sub> suspended solution. *J Hazard Mater* 157:300–307
- Boxall AB, Blackwell P, Cavallo R, Kay P, Tolls J (2002) The sorption and transport of a sulphonamide antibiotic in soil systems. *Toxicol Lett* 131:19–28
- Daughton CG, Ternes TA (1999) Pharmaceuticals and personal care products in the environment: agents of subtle change. *Environ Health Perspect* 107:907–938
- Lyon F (1994) IARC monographs on the evaluation of carcinogenic risks to humans. *Some Ind Chem* 60:389–433
- Belhamdi B, Merzougui Z, Trari M, Addoun A (2016) A kinetic, equilibrium and thermodynamic study of l-phenylalanine adsorption using activated carbon based on agricultural waste (date stones). *J Appl Res Technol* 14:354–366
- Bessekhouad Y, Brahimi R, Hamdini F, Trari M (2012) Cu<sub>2</sub>S/TiO<sub>2</sub> heterojunction applied to visible light Orange II degradation. *J Photochem Photobiol A : Chem* 248:15–23
- Boulahlib S, Boudina A, Si-Ahmed K, Bessekhouad Y, Trari M (2016) Development and validation of a fast and simple HPLC method for the simultaneous determination of aniline and its degradation products in wastewater. *Anal Methods* 8:5949–5956
- Lopez-Ramon MV, Stoeckli F, Moreno-Castilla C, Carrasco-Marin F (1999) On the characterization of acidic and basic surface sites on carbons by various techniques. *Carbon* 37:1215–1221
- Bouzaida I, Ferronato C, Chovelon JM, Rammah ME, Herrmann JM (2004) Heterogeneous photocatalytic degradation of the anthraquinonic dye, Acid Blue 25 (AB25): a kinetic approach. *J Photochem Photobiol A Chem* 168:23–30
- Perrin CL (2017) Linear or nonlinear least-squares analysis of kinetic data. *J Chem Educ* 94:669–672
- Urbansky ET (2001) Don't be tricked by your integrated rate plot. *J Chem Educ* 78:921–923
- Lente G (2004) Don't be tricked by your integrated rate plot: pitfalls of using integrated rate plots. *J Chem Educ* 81:82
- Vullier E, Chovelon JM, Guillard C, Herrmann JM (2003) Factors influencing the photocatalytic degradation of sulfonylurea herbicides by TiO<sub>2</sub> aqueous suspension. *J Photochem Photobiol A Chem* 159:71–79
- Boudiaf S, Nasrallah N, Mellal M, Belabed C, Belhamdi B, Meziani D, Mehdi B, Trari M (2020) Synthesis and characterization of semiconductor CoAl<sub>2</sub>O<sub>4</sub> for optical and dielectric studies: application to photodegradation of organic pollutants under visible light. *Optik* 219:165038. <https://doi.org/10.1016/j.jleo.2020.165038>
- Daghrir R, Drogui P (2013) Tetracycline antibiotics in the environment: a review. *Environ Chem Lett* 11(3):209–227. <https://doi.org/10.1007/s10311-013-0404-8>
- Subramonian W, Wu TY (2014) Effect of enhancers and inhibitors on photocatalytic sunlight treatment of methylene blue. *Water Air Soil Pollut* 225:1922. <https://doi.org/10.1007/s11270-014-1922-0>
- Fernández A, Lassaletta G, Jiménez VM, Justo A, González-Elipe AR, Herrmann JM, Tahiri H, Ait-ichou Y (1995) Preparation and characterization of TiO<sub>2</sub> photocatalysts supported on various rigid supports (glass, quartz and stainless steel). Comparative studies of photocatalytic activity in water purification. *Appl Catalysis B: Environ* 7:49–63
- Pouliquen H, Delépée R, Larhantec-Verdier M, Morvan M-L, Le Bris H (2007) Comparative hydrolysis and photolysis of four antibacterial agents (oxytetracycline oxolinic acid, flumequine and florfenicol) in deionised water, freshwater and seawater under abiotic conditions. *Aquaculture* 262:23–28
- Barka N, Assabbane A, Nounah A, Ichou YA (2008) Photocatalytic degradation of indigo carmine in aqueous solution by TiO<sub>2</sub>-coated non-woven fibres. *J Hazard Mater* 152:1054–1059
- Lazar MA, Varghese S, Nair SS (2012) Photocatalytic water treatment by titanium dioxide: recent updates. *Catalysts* 2:572–601
- Nosrati R, Olad A, Maramifar R (2012) Degradation of ampicillin antibiotic in aqueous solution by ZnO/polyaniline nanocomposite as photocatalyst under sunlight irradiation. *Environ Sci Pollut Res* 19:2291–2299
- Hapeshi E, Achilleos A, Vasquez MI, Michael C, Xekoukoulotakis NP, Mantzavinos D, Kassinos D (2010) Drugs degrading photocatalytically: kinetics and mechanisms of ofloxacin and atenolol removal on titania suspensions. *Water Res* 44:1737–1746



26. Sohrabi MR, Ghavami M (2008) Photocatalytic degradation of direct red 23 dye using UV/TiO<sub>2</sub>: effect of operational parameters. *J Hazard Mater* 153:1235–1239
27. Marci G, Augugliaro V, Lopez-Munoz MJ, Martin C, Palmisano L, Rives V, Schiavello M, Tilley RJ, Venezia AM (2001) Preparation characterization and photocatalytic activity of polycrystalline ZnO/TiO<sub>2</sub> systems. 2. Surface, bulk characterization, and 4-nitrophenol photodegradation in liquid–solid regime. *J Phys Chem B* 105:1033–1040
28. Galindo C, Jacques P, Kalt A (2000) Photodegradation of the aminoazobenzene acid orange 52 by three advanced oxidation processes: UV/H<sub>2</sub>O<sub>2</sub>, UV/TiO<sub>2</sub> and VIS/TiO<sub>2</sub>: comparative mechanistic and kinetic investigations. *J Photochem Photobiol A Chem* 130:35–47
29. Matos J, Garcia A, Cordero T, Chovelon JM, Ferronato C (2009) Eco-friendly TiO<sub>2</sub>-AC photocatalyst for the selective photooxidation of 4-chlorophenol. *Catal Lett* 130:568–574
30. Figueiredo JL, Pereira MFR (2010) The role of surface chemistry in catalysis with carbons. *Catal Today* 150(1–2):2–7
31. Wang W, Silva CG, Faria JL (2007) Photocatalytic degradation of Chromotrope 2R using nanocrystalline TiO<sub>2</sub>/activated-carbon composite catalysts. *Appl Catal B Environ* 70(1–4):470–478
32. Belhamdi B, Merzougui Z, Laksaci H, M. Trari (2019) The removal and adsorption mechanisms of free amino acid l-tryptophan from aqueous solution by biomass-based activated carbon by H<sub>3</sub>PO<sub>4</sub> activation: regeneration study. *Phys Chem Earth Parts A/B/C* 114, 102791
33. Haro M, Velasco LF, Ania CO (2012) Carbon-mediated photoinduced reactions as a key factor in the photocatalytic performance of C/TiO<sub>2</sub>. *Cat Sci Technol* 2:2264–2272
34. Velasco LF, Maurino V, Laurenti E, Fonseca IM, Lima JC, Ania CO (2013) Photoinduced reactions occurring on activated carbons. A combined photooxidation and ESR study. *Appl Catal A Gen* 452:1–8
35. Matos J, Laine J, Herrmann JM (2001) Effect of the type of activated carbons on the photocatalytic degradation of aqueous organic pollutants by UV-irradiated titania. *J Catal* 200:10–20
36. Herrmann JM, Matos J, Disdier J, Guillard C, Laine J, Malato S, Blanco J (1999) Solar photocatalytic degradation of 4-chlorophenol using the synergistic effect between titania and activated carbon in aqueous suspension. *Catal Today* 54:255–265
37. Matos J, Chovelon JM, Cordero T, Ferronato C (2009) Influence of surface properties of activated carbon on photocatalytic activity of TiO<sub>2</sub> in 4-chlorophenol degradation. *Open Environ Eng J* 2:21–29
38. Evgenidou E, Fytianos K, Poullos I (2005) Semiconductor-sensitized photodegradation of dichlorvos in water using TiO<sub>2</sub> and ZnO as catalysts. *Appl Catal B Environ* 59(1–2):81–89
39. Yang L, Yu LE, Ray MB (2009) Photocatalytic oxidation of paracetamol: dominant reactants, intermediates, and reaction mechanisms. *Environ Sci Technol* 43:460–465
40. Schulze-Hennings U, Bruckner I, Gebhardt W, Groteklaes M, Bloss SP, Wett M, Linnemann V, Montag D, Pinnekamp J (2017) Durability of a coating containing titanium dioxide for the photocatalytic degradation of diclofenac in water with UV-A irradiation. *Water Environ J* 31:508–514
41. Cordero-Garcia A, Guzman-Mar JL, Hinojosa-Reyes L, Ruiz-Ruiz E, Hernandez-Ramirez A (2016) Effect of carbon doping on WO<sub>3</sub>/TiO<sub>2</sub> coupled oxide and its photocatalytic activity on diclofenac degradation. *Ceram Int* 42:9796–9803
42. Leary R, Westwood A (2011) Carbonaceous nanomaterials for the enhancement of TiO<sub>2</sub> photocatalysis. *Carbon* 49:741–772
43. Ania CO, Velasco LF, Valdés-Solís T (2012) Photochemical behavior of carbon adsorbents. In: Tascón JMD (ed) *Novel carbon adsorbents*. Elsevier, Oxford, pp 521–547
44. Kleinwechter H, Janzen C, Knipping J, Wiggers H, Roth P (2002) Formation and properties of ZnO nano-particles from gas phase synthesis processes. *J Mater Sci* 37:4349–4360
45. Raza W, Haque M, Muneer M (2014) Synthesis of visible light driven ZnO: characterization and photocatalytic performance. *Appl Surf Sci* 322:215–224
46. Anandan S, Vinu A, Lovely KS, Gokulakrishnan N, Srinivasu P, Mori T, Murugesan V, Sivamurugan V, Ariga K (2007) Photocatalytic activity of La-doped ZnO for the degradation of monocrotophos in aqueous suspension. *J Mol Catal A Chem* 266:149–157

## Authors and Affiliations

**Assia Djebri<sup>1</sup> · Mohamed Belmedani<sup>2</sup> · Badreddine Belhamdi<sup>3</sup> ·  
Mohamed Trari<sup>4</sup> · Zahra Sadaoui<sup>1</sup>**

- <sup>1</sup> Faculty of Mechanical and Processes Engineering, Laboratory of Reaction Engineering, BP 32, 16111 Algiers, Algeria
- <sup>2</sup> Faculty of Mechanical and Processes Engineering, Laboratory of transfer phenomena, BP 32, 16111 Algiers, Algeria
- <sup>3</sup> Laboratory of Physical and Chemical Study of Materials and Applications in the Environment, Faculty of Chemistry University USTHB, BP 32, 16111 Algiers, Algeria
- <sup>4</sup> Laboratory of Storage and Valorization of Renewable Energies, Faculty of Chemistry University USTHB, BP 32, 16111 Algiers, Algeria